N^6-methyladenosine binding proteins negatively regulate HIV-1 infectivity and viral production

Wuxun Lu [1], Nagaraja Tirumuru [1], Pratibha C. Koneru [2], Chang Liu [3, 4], Mamuka Kvaratskhelia [2], Chuan He [3, 4], and Li Wu [1, *]

[1] Center for Retrovirus Research, Department of Veterinary Biosciences, The Ohio State University, Columbus, Ohio 43210, USA

[2] Division of Infectious Diseases, University of Colorado School of Medicine, Aurora, Colorado 80045, USA

[3] Department of Chemistry, Department of Biochemistry and Molecular Biology, Institute for Biophysical Dynamics, The University of Chicago, Chicago, Illinois 60637, USA

[4] Howard Hughes Medical Institute, The University of Chicago, Chicago, Illinois 60637, USA

Email addresses for all authors

Wuxun Lu: lu.1656@osu.edu

Nagaraja Tirumuru: tirumuru.1@osu.edu

Pratibha C. Koneru: pratibha.koneru@ucdenver.edu

Chang Liu: changliu@uchicago.edu

Mamuka Kvaratskhelia: mamuka.kvaratskhelia@ucdenver.edu

Chuan He: chuanhe@uchicago.edu

Li Wu: wu.840@osu.edu

[*]Correspondence author: Li Wu

Abstract

Background: The internal N^6-methyladenosine (m^6A) modification of cellular mRNA regulates post-transcriptional gene expression. The YTH domain family proteins (YTHDF1-3, or Y1-3) bind to m^6A-modified cellular mRNA and modulate its metabolism and processing, thereby affecting protein translation in cells. We previously reported that HIV-1 RNA contains m^6A modification and that Y1-3 proteins inhibit HIV-1 infection by decreasing HIV-1 reverse transcription. Here we extended our studies to further understand the mechanisms of Y1-3-mediated inhibition of HIV-1 infection and viral production.

Results: Overexpression of Y1-3 proteins in HIV-1 target cells decreased viral genome RNA (gRNA) levels and inhibited early and late reverse transcription. Purified recombinant Y1-3 proteins preferentially bound to the m^6A-modified 5' leader sequence of gRNA compared with its unmodified RNA counterpart, consistent with the strong binding of Y1-3 to HIV-1 gRNA in infected cells. HIV-1 mutants with two altered m^6A modification sites in the 5' leader sequence of gRNA demonstrated significantly lower infectivity compared with wild-type HIV-1, confirming that these sites are important for viral infection. HIV-1 produced from cells with knockdown of endogenous Y1, Y3, or Y1-3 proteins together showed increased viral infectivity compared with HIV-1 produced from control cells. Interestingly, we found that Y1-3 proteins and HIV-1 Gag formed a complex with RNA in HIV-1-infected target cells.

Conclusions: Our results suggest the inhibitory effects of Y1-3 proteins on HIV-1 infection and provide new insight into the mechanisms of m^6A modification of HIV-1 RNA in regulating viral replication, which clarify some discrepancies in the previously published studies in this area.

Keywords: HIV-1 infection, HIV-1 production, RNA m^6A modification, m^6A-binding proteins

47 **Background**

48 Among the more than 100 distinct modifications identified in mRNAs in different
49 organisms, N^6-methyladenosine (m^6A) methylation is the most prevalent internal modification,
50 accounting for 0.1% of adenosines in mammalian mRNAs [1]. The dynamic addition, removal,
51 and recognition of m^6A in cellular RNAs are coordinately regulated by three groups of host
52 proteins, including methyltransferases (termed writers), demethylases (erasers), and m^6A-binding
53 proteins (readers). The writers include methyltransferase-like 3 (METTL3), methyltransferase-
54 like 14 (METTL14), and Wilms tumor 1-associated protein (WTAP), while erasers include fat
55 mass and obesity-associated protein (FTO) and alkB homologue 5 (ALKBH5) [2]. The readers
56 are YT521-B homology (YTH) domain family proteins (YTHDF1, YTHDF2, YTHDF3 and
57 YTHDC1) that specifically recognize m^6A modification via a conserved m^6A-binding pocket in
58 the YTH domain [3-5]. These reader proteins modulate m^6A-modifed mRNA stability and
59 translation, therefore playing an important role in modulating post-transcriptional gene
60 expression [6-10].

61 Three recent studies highlighted the importance of m^6A modifications of HIV-1 RNA in
62 regulating viral replication and gene expression [11-13]. Despite some consistent results, there
63 are discrepancies in the locations, effects, and mechanisms of m^6A modification of HIV-1 RNA
64 in these studies [11-13]. Our published study identified m^6A modifications in the 5' and 3' un-
65 translated regions (UTRs), as well as in the *rev* and *gag* genes of the HIV-1 genome [13]. We
66 previously reported that overexpression of Y1-3 proteins in cells inhibits HIV-1 infection by
67 primarily decreasing HIV-1 reverse transcription, while knockdown of endogenous Y1-3 in
68 Jurkat $CD4^+$ T-cell line or primary $CD4^+$ T-cells increases HIV-1 infection [13]. However, the
69 underlying mechanisms of Y1-3-mediated inhibition of HIV-1 infection remain unclear.

70 Here we report that Y1-3 inhibited HIV-1 infection in target cells by lowering viral
71 genome RNA (gRNA) levels and reverse transcription products. We demonstrate that the m^6A-
72 modified HIV-1 RNA fragment preferentially bound to Y1-3 proteins compared with an un-
73 modified RNA counterpart, and mutations of two m^6A sites in the 5' UTR significantly
74 decreased viral infectivity. Knockdown of endogenous Y1, Y3 or Y1-3 proteins together in
75 virus-producing cells positively modulated HIV-1 infectivity. Furthermore, we found that
76 endogenous Y1-3 proteins and HIV-1 Gag protein formed a complex with RNAs in HIV-1-
77 infected target cells. Together, these findings suggest new mechanisms by which Y1-3 proteins
78 mediate HIV-1 inhibition during early steps of the viral life cycle.
79
80 **Results**
81 **Overexpression of Y1-3 proteins in target cells inhibits post-entry HIV-1 infection by**
82 **decreasing HIV-1 gRNA level and inhibiting viral reverse transcription**
83 Our previous study showed that Y1-3 proteins negatively regulate HIV-1 post-entry
84 infection in target cells, including primary $CD4^+$ T-cells [13]. To better understand the
85 underlying mechanisms, we compared HIV-1 gRNA levels, early and late reverse transcription
86 (RT) products in cells overexpressing individual Y1-3 proteins and control cells after HIV-1
87 infection. We first used vesicular stomatitis virus glycoprotein (VSV-G)-pseudotyped single-
88 cycle HIV-1 expressing firefly luciferase to infect HeLa cells stably expressing each individual
89 Y1-3 proteins (HeLa/Y1-3) or control cells transduced with an empty vector (HeLa/Vector).
90 Consistent with our previous results [13], Y1-3 overexpression (Fig. 1A) resulted in significantly
91 lower levels of HIV-1 post-entry infection (26%, 8.6%, and 23% in HeLa/Y1, HeLa/Y2 and
92 HeLa/Y3 cells, respectively) compared with HeLa/Vector control cells (set as 100%, Fig. 1B).

93 To examine whether Y1-3 proteins alter the levels of HIV-1 gRNA in the infected cells,
94 HeLa/Y1-3 or control cells were infected with single-cycle HIV-1 and total RNAs from the cells
95 were isolated at 1, 3, and 6 h post-infection (hpi). The levels of HIV-1 gRNA were quantified
96 using RT-qPCR [14]. At each time point tested, HIV-1 gRNA levels were lower in HeLa/Y1-3
97 relative to those in HeLa/Vector control cells, and HIV-1 gRNA level gradually declined after
98 infection as expected (Fig. 1C). These results indicate that overexpression of Y1-3 proteins leads
99 reduced levels of HIV-1 gRNA, likely by decreasing viral RNA stability.
100 Our previous study showed that Y1-3 proteins inhibit accumulation of HIV-1 late RT
101 products in infected cells [13]; however, it is unclear whether Y1-3 proteins affect HIV-1 early
102 RT efficiency. To address this question, HeLa/Y1-3 cells or HeLa/Vector control cells infected
103 by HIV-1-Luc/VSV-G were collected at 6, 12 and 24 hpi for quantification of HIV-1 early and
104 late RT products by quantitative PCR (qPCR) [15]. At each time point, the levels of both early
105 and late RT products were significantly lower in HeLa/Y1-3 cells compared with vector control
106 cells (Fig. 1D and 1E). Compared with vector control cells at 6 hpi, Y1-3 overexpression
107 decreased HIV-1 gRNA levels, and further decreased early and late RT products (Fig. 1C-E),
108 suggesting that overexpression of Y1-3 proteins decreases viral gRNA stability and inhibits early
109 RT product synthesis. At 24 hpi, the levels of early and late RT products decreased to 37-54%,
110 while HIV-1 infection decreased to 8.6-26% in HeLa/Y1-3 cells compared with vector control
111 cells (set to 100% in Fig. 1B, 1D and 1E). Together, these results suggest that overexpression of
112 Y1-3 proteins in target cells inhibits HIV-1 infection mainly by decreasing HIV-1 gRNA level
113 and inhibiting viral reverse transcription.
114

115 **Overexpression of Y1-3 proteins in HeLa/CD4 target cells inhibits wild-type (WT) HIV-1**
116 **replication**

117 Since the *firefly luciferase* gene in HIV-1-Luc/VSV-G virus has consensus sequences
118 recognized by m^6A writers, its mRNA may also have m^6A modifications. To exclude the effects
119 of m^6A modification of *luciferase* mRNA on HIV-1 infection, we used WT, replication-
120 competent HIV-1_{NL4-3} to infect HeLa cells overexpressing CD4 and individual Y1-3 proteins
121 (HeLa/CD4/Y1-3) or vector control cells. Using flow cytometry, we confirmed that the majority
122 of these cells were double positive for the HIV-1 primary receptor CD4 and co-receptor CXCR4
123 (71-81%), which would allow efficient fusion-mediated viral entry (Fig. 2A). Immunoblotting
124 results also confirm that HeLa/CD4/Y1-3 cells stably expressed FLAG-tagged individual Y1-3
125 proteins (Fig. 2B).

126 In order to examine the effects of Y1-3 overexpression on HIV-1 replication in the full
127 viral lifecycle, we collected infected cells or supernatants at 72 hpi for further analyses (Fig. 2B-
128 F). Consistent with the results from single-cycle HIV-1-Luc/VSV-G (Fig. 1B), Y1-3
129 overexpression efficiently inhibited infection of WT HIV-1_{NL4-3} as Gag protein levels in cells
130 and p24 (capsid) levels in supernatants were significantly lower in HeLa/CD4/Y1-3 cells
131 compared with vector control cells (Fig. 2B and 2C). These results confirmed inhibitory effects
132 of Y1-3 proteins on HIV-1 infection, and suggested that the inserted *luciferase* gene in HIV-1-
133 Luc/VSV-G does not affect the observed phenotype. Infection of HeLa cells overexpressing Y1-
134 3 proteins with WT HIV-1 also resulted in significantly lower early and late HIV-1 RT products
135 (Fig. 2D and 2E, respectively), and consequently reduced *gag* mRNA levels compared with
136 vector control cells (Fig. 2F). These data suggest that Y1-3 proteins inhibit WT HIV-1_{NL4-3}
137 infection before or during the RT stage.

138

139 **Y1-3 proteins specifically bind to HIV-1 gRNA in infected HeLa/CD4 cells**

140 To confirm Y1-3 binding to HIV-1 gRNA in infected cells, we performed
141 immunoprecipitation (IP) of Y1-3 in HeLa/CD4/Y1-3 cell lines and vector control cells infected
142 with WT HIV-1_{NL4-3} (Fig. 3A). To validate the specificity of Y1-3 binding to HIV-1 RNA, we
143 also included a Y1-3 unrelated cellular protein MAL (MyD88 adapter-like, also known as
144 Toll/IL-1 receptor (TIR) domain-containing adapter protein, or TIRAP) [16, 17] as an additional
145 negative control in the IP assay (Fig. 3A). We then quantified the amounts of Y1-3-bound HIV-1
146 gRNA using RT-qPCR assays [13]. We observed that Y1-3 specifically and efficiently bound to
147 WT HIV-1 gRNA in HIV-1_{NL4-3} infected HeLa/CD4/Y1-3 cells compared with vector control or
148 MAL-expressing cells (Fig. 3B). The levels of HIV-1 gRNA bound to Y1 appeared higher than
149 those bound to Y2 and Y3 (Fig. 3B), which could be due to the higher expression of Y1 in
150 HeLa/CD4 cells relative to Y2 and Y3 proteins (Fig. 3A) and consequently a higher level of IP
151 products (Fig. 3B). These data confirm that Y1-3 proteins specifically bind to WT HIV-1_{NL4-3}
152 gRNA in infected cells.

153

154 **Purified recombinant Y1-3 proteins preferentially bind to an m^6A-modifed HIV-1 RNA**
155 **fragment *in vitro*.**

156 Our previous study showed that HIV-1 RNA contains m^6A modifications at both the 5' and 3'
157 UTR [13]. Given the critical role of the 5' UTR in initiation of HIV-1 reverse transcription, in
158 this study we focused on the m^6A sites in the 5' UTR of HIV-1 gRNA. The GGACU motif is the
159 most predominant sequence for m^6A modification [18, 19]. The m^6A peak detected by high-
160 throughput RNA sequencing in the 5' UTR of HIV-1 gRNA harbors two GGACU motifs [13].

161 The first one is located in the primer-binding site (PBS), and the second is in upstream region of
162 the dimer initiation sequence (DIS) (Fig. 4A). These two GGACU motifs overlap with m^6A
163 modifications in HIV-1 gRNA and are close to Y1-3 protein-binding peaks identified in the 5'
164 UTR of HIV-1 gRNA [13].

165 To study the binding properties of Y1-3 proteins to HIV-1 RNA with m^6A modification,
166 we synthesized two RNA fragments corresponding to nucleotides 235-281 of HIV-1_{NL4-3} gRNA
167 with or without m^6A modification in the second GGACU motif located in the 5' UTR (Fig. 4A).
168 To eliminate RNA dimerization in our binding assays, the underlined DIS sequence
169 (AAGCGCGC) was replaced with the nucleotides GAG (Fig. 4A and 4B). We first used the
170 AlphaScreen assay [20] to detect interaction of synthesized RNA fragments with purified full-
171 length recombinant Y1-3 proteins. Each of these Y1-3 proteins exhibited clear preference for
172 binding to m^6A-modified HIV-1 RNA than its unmodified counterpart (Fig. 4C). We further
173 investigated *in vitro* binding of the RNA fragments to Y1-3 protein using affinity pull-down
174 experiments. Streptavidin-conjugated beads were used to pull-down biotin-modified control or
175 m^6A RNA fragments. Consistently, at lower Y1-3 concentrations (1-25 nM), clear preferences
176 were seen for binding to m^6A-modified HIV-1 RNA relative to control RNA, though both RNA
177 fragments had detectable binding to Y1-3 proteins at higher concentrations (125-625 nM) (Fig.
178 4D). The immunoblotting results of the pull-down experiments were quantified and normalized
179 to 1 based on protein pull-down levels by m^6A RNA fragment at 625 nM protein input (Fig. 4E).
180 To compare affinity of RNA fragments to Y1-3 proteins, we calculated the concentrations of
181 each Y1-3 protein (ranging from 1-625 nM) required for 50% pull-down levels based on the
182 regression curves (Fig. 4E and 4F). The 50% pull-down efficiencies indicated that Y1-3 proteins
183 bound to m^6A RNA fragment 7-fold, 13-fold, and >20-fold higher than control RNA,

184 respectively (Fig. 4F). These results demonstrate that Y1-3 proteins exhibit substantially higher
185 affinity for m^6A-modified HIV-1 RNA *in vitro*, which may contribute to Y1-3-mediated
186 inhibition of HIV-1 infection in cells.
187
188 **A to G mutations in GGACU motifs of the 5' UTR of HIV-1 gRNA reduce viral infectivity**
189 The two GGACU motifs are located in the PBS and an upstream region of the DIS (Fig.
190 4A), within the m^6A peaks of the 5' UTR of HIV-1 RNA that were identified in our previous
191 study [13]. Because the 5' UTR is critical for HIV-1 reverse transcription, genome package, and
192 viral infectivity [21, 22], we further investigated the importance of these m^6A sites on HIV-1
193 replication and infection by mutagenesis. To eliminate m^6A modification of the GGACU motifs
194 in HIV-1 gRNA, A to G mutations were introduced in the first (Mut1), second (Mut2), or both
195 GGACT motifs (Mut3) in the HIV-1 proviral DNA plasmid pNL4-3 (Fig. 5A). WT pNL4-3 and
196 derived mutants (Mut1-3) were separately transfected into HEK293T cells to measure HIV-1
197 protein expression and viral release. Compared with WT HIV-1, these mutants expressed
198 comparable levels of precursor Gag protein, but the levels of cleaved p24 and intermediate Gag
199 products in cell lysates were 1.4- to 1.8-fold higher (Fig. 5B). Consistently, supernatant p24
200 levels of mutant viruses were 1.2- to 1.4-fold higher than that of WT HIV-1 (Fig. 5C), suggesting
201 a potential effect of these mutations on Gag proteolytic processing or viral release. To compare
202 the infectivity of the mutants with WT HIV-1, viruses generated in HEK293T cells with equal
203 amounts of p24 were used to infect TZM-bl indicator cells [23]. Interestingly, the infectivity of
204 the mutant viruses was significantly lower (53-74%) relative to WT HIV-1 (Fig. 5D), suggesting
205 an important role of these two GGACU motifs in HIV-1 infectivity.

206 Previously published m^6A mapping results indicate that there are multiple m^6A sites in
207 different regions of HIV-1 gRNA in addition to the 5' UTR [11-13], which can potentially
208 contribute to regulating viral infectivity through interactions with Y1-3 proteins. To address this,
209 we examined whether silencing Y1-3 in target cells could restore the infectivity of these 5' UTR
210 mutant viruses. Endogenous Y1-3 proteins in TZM-bl cells were knocked down by combined
211 Y1-3 specific siRNA, and then TZM-bl cells were infected with the same p24 amount of WT or
212 mutant viruses generated from normal HEK293T cells. In TZM-bl target cells with partial Y1-3
213 proteins knockdown (Fig. 5E), all three mutant viruses showed 40-50% lower infectivity relative
214 to WT HIV-1 (Fig. 5F). These results confirm the importance of these two GGACU motifs for
215 HIV-1 infectivity, and suggest that other m^6A sites in HIV-1 RNA can also regulate viral
216 infectivity.
217 Given the important role of the PBS and DIS in structure and function of HIV-1 gRNA
218 [24], we predicted the secondary structures of the RNA segments containing the PBS and DIS of
219 WT and mutant viruses. Compared with the structure of WT HIV-1, the A to G mutation in the
220 first GGACU motif (Mut1) resulted in a longer stem structure in the PBS sequence region, while
221 mutation in the second GGACU motif did not change RNA structure containing the DIS (Fig.
222 5G). These results suggest that the decreased viral infectivity of Mut1 might be due to the
223 combined effects of RNA structure change and elimination of m^6A at this site. In contrast, the
224 reduced viral infectivity of Mut2 was likely due to elimination of m^6A modification.
225
226 **Y1-3 protein knockdown in virus-producing cells decreases HIV-1 Gag expression and**
227 **alters viral production and infectivity**

228 Our published results [13] and new data showed that Y1-3 proteins in target cells
229 negatively regulate single-cycle and replication-competent HIV-1 infection (Fig. 1B and 2B-C,
230 respectively). To further elucidate the role of Y1-3 in HIV-1 protein expression and infectivity,
231 endogenous Y1-3 gene expression in virus-producing HEK293T cells was knocked down using
232 specific siRNAs. Compared with non-specific control siRNA, single knockdown of each Y1-3
233 significantly decreased HIV-1 Gag (Pr55) protein expression, and correspondingly reduced the
234 levels of processed p24 protein in cells (Fig. 6A). Consistently, p24 levels in the supernatants of
235 cells with single or combined Y1-3 knockdown also reduced approximately 2-fold compared
236 with those of control cells, and there was no synergistic effect of combined knockdown (Fig.
237 6B).
238 To compare the infectivity of HIV-1 generated from cells with Y1-3 knockdown, viruses
239 with equal amounts of p24 were used to infect TZM-bl indicator cells. As shown in Fig. 6C,
240 HIV-1 generated from individual Y1 or Y3 knockdown cells had significantly higher infectivity
241 compared with virus from control cells ($P < 0.005$), suggesting that Y1 and Y3 proteins in cells
242 negatively affect infectivity of progeny HIV-1. In contrast, efficient Y2 knockdown in virus-
243 producing cells resulted in a 25% decrease in HIV-1 infectivity (Fig. 6A and 6C), suggesting a
244 different mechanism of Y2-mediated inhibitory effect on viral infection. Moreover, combined
245 Y1-3 knockdown efficiently reduced endogenous levels of Y1-3 proteins in virus-producing cells
246 (Fig. 6A, last lane), but only modestly increased HIV-1 infectivity (Fig. 6C), which were likely
247 due to the different effects resulting from Y1/3 and Y2 knockdown.
248
249 **Y1-3 proteins and HIV-1 Gag form a complex with RNAs in HIV-1-infected target cells**

250 To examine whether Y1-3 could interact with any HIV-1 proteins in cells, we performed
251 IP of overexpressed Y1-3 in HEK293T cells co-transfected with pNL4-3, and then detected HIV-
252 1 proteins in the input and IP products by immunoblotting using human anti-HIV-1
253 immunoglobulin [25]. Interestingly, we found that Y1-3 co-precipitated with HIV-1 Gag (Pr55)
254 and intermediate Gag products, but not with HIV-1 p24 (Fig. 7, lanes labeled with IP). The
255 vector cells were used as a negative control for IP and showed a background band of Gag (Pr55)
256 in the IP product (Fig. 7, lane 2 from the left). Immunoblotting of FLAG confirmed expression
257 and IP of FLAG-tagged Y1-3 proteins in the transfected cells. Because both Y1-3 proteins and
258 HIV-1 Gag can bind cellular and HIV-1 RNAs [8, 10, 13, 26], to examine whether RNAs
259 mediate the association between Gag and Y1-3 proteins, cell lysates were treated with RNase A
260 before IP. Interestingly, RNase A treatment completely eliminated HIV-1 Gag signal in Y1-3
261 precipitation (Fig. 7, lanes labeled with RNase + IP). These results suggest that Y1-3 proteins
262 and HIV-1 Gag form a complex with RNAs in cells.
263

264 **Discussion**

265 Reversible m^6A modification is the most prevalent mRNA modification in eukaryotic organisms,
266 and plays critical roles in gene expression [5]. Although m^6A modification was previously
267 identified in different viruses [27-29], its roles in HIV-1 gene expression regulation were
268 recently recognized [11-13]. While these studies identified specific m^6A sites in HIV-1 gRNA,
269 they disagreed on the extent and locations of m^6A modifications along the HIV-1 genome and
270 their effects on viral replication [11-13]. Lichinchi *et al.* [11] reported 14 peaks of m^6A
271 modification in HIV-1 RNA, in which the m^6A modification in the Rev response element region
272 increased binding to Rev and facilitated nuclear export of viral RNA, thereby enhancing HIV-1

273 replication. In contrast, Kennedy *et al.* [12] found 4 clusters of m^6A modification in the 3' UTR
274 region of HIV-1 RNA. Our study showed that HIV-1 gRNA has m^6A modifications in the 5' and
275 3' UTRs as well as *gag* and *rev* genes [13]. Also, there is controversy regarding the roles of Y1-3
276 proteins in HIV-1 replication. In the presence of Y1-3 overexpression, Kennedy *et al*. observed
277 increased HIV-1 replication [12], while our data showed decreased HIV-1 replication [13]. These
278 discrepancies could stem from different cell types or lines, reagents, and techniques used, and
279 need to be further investigated. In this study, we demonstrated that Y1-3 proteins suppress HIV-1
280 single-cycle and spreading infection in cells by decreasing viral gRNA and RT products. Y1-3
281 overexpression in HIV-1 infected cells led to significantly lower levels of early and late RT
282 product, and further decreased HIV-1 infectivity, suggesting that Y1-3 proteins could also inhibit
283 other steps after reverse transcription during the HIV-1 life cycle.

284 The GGACU is the predominant sequence in RRACH (R=G or A; H=A, C or U) motif
285 recognized by the m^6A writers [30]. Our *in vitro* biochemical experiments reveal that Y1-3
286 proteins exhibit clear preference for the m^6A-modified HIV-1 RNA fragment over its unmodified
287 RNA counterpart. The preferential binding of m^6A sites in the HIV-1 genome to Y1-3 proteins
288 may contribute to decreased HIV-1 infection in HeLa/Y1-3 cells. There are two GGACU motifs
289 in the 5' UTR of HIV-1_{NL4-3} gRNA. The first GGACU motif is in the PBS region, and is
290 conserved in HIV-1 and simian immunodeficiency virus (SIV) [31], suggesting critical roles of
291 the motif in HIV-1 and SIV life cycles. The second GGACU motif is in the DIS stem. This motif
292 is conserved in HIV-1 subtype B isolates, but A to G mutations can be found in subtype C and
293 group O isolates (https://www.hiv.lanl.gov/).

294 Compared with WT viruses, mutant viruses harboring A to G mutations have
295 significantly reduced infectivity. We noted that the first GGACU motif is in the PBS and

296 mutation at this site in Mut 1/3 viruses (A to G at nt. 197) introduces a mismatch with $tRNA^{lys}$
297 primer [32], which may affect primer annealing and therefore impair viral infectivity. Recent
298 studies showed that the second GGACU motif interacts with HIV-1 nucleocapsid (NC) protein in
299 viral particles [32], and that nucleotides GGA in this motif strongly bind Gag precursor for viral
300 genome packaging [33]. Mutation at this site may also impair interactions between HIV-1 gRNA
301 and NC protein, contributing to decreased infectivity in mutant viruses. Thus, the decreased
302 infectivity of Mut2 and Mut3 viruses (A to G at nt. 241) may be due to eliminated m^6A
303 modification at the second GGACU motif and/or decreased interactions between HIV-1 gRNA
304 and Gag/NC. The effects of these mutations on primer binding and Gag/NC interactions remain
305 to be examined.

306 Y1-3 proteins specifically recognizing m^6A sites via a hydrophobic pocket in the YTH
307 domain [3]. The effects of Y1-3 on HIV-1 gene expression, viral production in virus-producing
308 HEK293T cells and infectivity of progeny HIV-1 appear complex. Individual or combined
309 knockdown of each endogenous Y1-3 decreased HIV-1 Gag expression in cells and virion
310 release in the supernatants (Fig. 6A and 6B). Knockdown of endogenous Y1 or Y3 proteins in
311 virus-producing increased progeny HIV-1 infectivity, while Y2 knockdown modestly reduced
312 the infectivity of progeny HIV-1 (Fig. 6C). These results together suggest that, in virus-
313 producing cells, endogenous Y1-3 proteins positively regulate HIV-1 Gag protein expression,
314 while Y1 and Y3 proteins negatively affect infectivity of the progeny HIV-1. Furthermore, the
315 m^6A modification regulates RNA processing and stability [2, 5, 34]. After HIV-1 transcription,
316 viral RNA undergoes extensive splicing to express structural and accessory proteins. The roles of
317 m^6A modification in HIV-1 RNA splicing, stability and dimerization remain to be elucidated.

318 In addition to HIV-1, recent studies have identified viral RNA m^6A modifications and its
319 roles in regulating replication of *Flaviviridae* viruses, including hepatitis C virus (HCV), dengue,
320 Zika virus (ZIKV), yellow fever virus, and West Nile virus [35, 36], Kaposi's sarcoma-
321 associated herpesvirus (KSHV) [37, 38], and influenza A virus (IAV) [39]. The m^6A
322 modification in viral RNA increases RNA expression of IAV [39], promotes KSHV lytic
323 replication [37], but negatively regulates HCV and ZIKV production [35, 36]. Similar to our
324 findings that Y1-3 proteins inhibit HIV-1 infection [13], Y1-3 proteins also negatively regulate
325 HCV and ZIKV replication [35, 36]. A more recent study reported that Y2 protein negatively
326 regulates the KSHV lytic replication by enhancing decay of KSHV transcripts [38]. Y1 and Y3
327 have no effect on IAV infection, while Y2 overexpression significant enhances IAV gene
328 expression and replication [39]. Although different approaches in these studies may account for
329 discrepancies, these results suggest that m^6A modification and Y1-3 proteins have distinct effects
330 on various viruses.
331
332 **Conclusions:** We found that m^6A reader proteins Y1-3 inhibit HIV-1 infection by decreasing
333 viral gRNA and early reverse transcription products. We demonstrate that Y1-3 proteins
334 preferentially bind to m^6A-modified HIV-1 RNA. Mutation of m^6A sites in the 5' UTR resulted
335 in decreased viral infectivity, suggesting important roles of these sites for HIV-1 infection. Y1-3
336 proteins and HIV-1 Gag form a complex with RNAs in virus-producing cells. Together, these
337 results help better understand the roles and mechanisms of m^6A modification of HIV-1 RNA in
338 regulating viral replication.
339
340 **Methods**

341 **Cell culture**. HEK293T cell line (a kind gift from Dr. Vineet KewalRamani, National Cancer
342 Institute, Frederick, USA) and TZM-bl cells [[23] obtained through the NIH AIDS Reagent
343 Program, Catalog # 8129] were maintained in complete DMEM as described [40]. HeLa or
344 HeLa/CD4 cell lines (kind gifts from Dr. Vineet KewalRamani, National Cancer Institute,
345 Frederick, USA) overexpressing empty vector (pPB-CAG), individual FLAG- and HA-tagged
346 Y1, Y2 or Y3 protein were maintained in complete DMEM containing 2 μg/mL puromycin as
347 described [13].
348
349 **Generating HeLa cell lines stably express CD4 and Y1-3 proteins.** HeLa/CD4 cells were
350 generated by transduction of HeLa cells with a pMX retroviral vector expressing human CD4
351 [41]. HeLa/CD4 cells were transfected separately with pPB-CAG vector-based Y1-3 expressing
352 constructs or pPB-CAG empty vector, and then selected with puromycin (2 μg/mL). HeLa/CD4
353 stably expressing cells Y1-3 were cultured as described [13].
354
355 **Mutagenesis in HIV-1 proviral DNA plasmid (pNL4-3).** Mutations in pNL4-3 were
356 introduced using Agilent QuickChange Lightning Multi Site-directed Mutagenesis Kit (catalog #
357 210515-5) according to the instructions. Primers mut1 (5'-CCCGAACAGGGGCTTGAAAGC-
358 3') and mut2 (5'-TCGACGCAGGGCTCGGCTTG-3') were used (mutation sites are underlined)
359 to generate A to G mutation at the first (nt. 197), the second (nt. 241) or both GGACU motifs
360 between HIV-1 gRNA U5 and *gag* gene. The mutations were confirmed by DNA sequencing.
361
362 **siRNA knockdown of Y1-3 proteins.** Y1-3 expressions were knocked down by two rounds of
363 siRNA transfection using specific siRNAs (QIAGEN) and Lipofectamine RNAiMax

364 (Invitrogen) according to instructions (siRNA sequences are listed in Table 1). Briefly,
365 HEK293T cells (1.5×10^5 per well) in 24-well plates were transfected with gene specific siRNAs
366 or control siRNA. Twenty-four h after transfection, cell culture media were replaced and the
367 second-round siRNA transfection was conducted. At 6 h after the second round of siRNA
368 transfection, pNL4-3 (0.5 μg per well) was transfected to HEK293T cells. Cells and culture
369 media were collected at 36 h after pNL4-3 transfection for immunoblotting, p24 quantification,
370 and infection assays.
371
372 **HIV-1 stocks and infection assays.** Single-cycle HIV-luc/VSV-G was generated as previously
373 described [13]. Replication-competent WT and mutant HIV-1 stocks were generated by
374 transfection of HEK293T cells with pNL4-3 or mutant proviral DNA plasmids using
375 Lipofectamine 2000 (Invitrogen) according to instructions. For Y1-3 and pNL4-3 co-expression
376 experiments, pPB-CAG vector or pPB-CAG expressing individual FLAG- and HA- tagged Y1-3
377 protein was transfected into HEK293T cells, and pNL4-3 proviral DNA was transfected 12 h
378 later. At 48 h (WT and Mut1-3 plasmids) or 36 h (Y1-3 co-expression) after proviral DNA
379 transfection, cells were collected for immunoblotting and HIV-1 capsid p24 levels in viral stocks
380 were quantified by an enzyme-linked immunosorbent assay (ELISA) using anti-p24-coated
381 plates (AIDS and Cancer Virus Program, NCI-Frederick, MD) as described [13, 41]. To compare
382 infectivity of WT HIV-1 in HeLa/Y1-3 cells, HIV-luc/VSV-G was used for infection at
383 multiplicity of infection (MOI) at 1 as described [13]. To compare the infectivity of WT HIV-
384 1_{NL4-3} and mutant viruses, viruses with equal amounts of p24 (400 pg) were used to infect TZM-
385 bl cells in 24-well plates. At 48 hpi, TZM-bl cells were washed twice with PBS and lysed for
386 luciferase assay (Promega) according to the manufacturer's instructions. Cell protein

387 concentrations were quantified using a bicinchoninic acid assay (Pierce) and all luciferase results
388 were normalized based on total protein input.
389
390 **Flow cytometry measure cell surface levels of CD4 and CXCR4.** HeLa/CD4 cells were
391 treated with the non-enzymatic cell dissociation solution (C5914, Sigma-Aldrich) and double
392 stained with FITC-conjugated CD4 (MHCCD0401-4, Thermo Fisher) and phycoerythrin-
393 conjugated CXCR4 (555974, BD Pharmingen) antibodies as described [13]. Cells stained with a
394 mouse IgG2a isotype antibody (555574, BD Pharmingen) were used as a negative control. Flow
395 cytometry was analyzed using a Guava EasyCyte Mini and data analysis was performed using
396 FlowJo (FlowJo, LLC) software as described [42].
397
398 **IP of Y1-3 proteins and RT-qPCR detection of HIV-1 gRNA.** HeLa/CD4 cells expressing
399 MAL were generated by transfection with pEF-Bos MAL Flag (plasmid # 41554 from Addgene)
400 [17]. HeLa/CD4 cells expressing pPB-CAG vector, MAL or Y1-3 proteins (3×10^6 cells) were
401 seeded in a 60 mm-diameter culture plate one day before HIV-1 infection. Cells were infected
402 with HIV-1_{NL4-3} at a multiplicity (MOI) of infection of 5 for 3 h. Cells were UV-cross-linked and
403 lysed in cell lysis buffer (Sigma-Aldrich). Co-immunoprecipitated RNA was isolated and RT-
404 qPCR quantification of HIV-1 gRNA was performed as described [13].
405
406 **Antibodies and immunoblotting.** Antibodies used in this study were: anti-GAPDH (clone 4G5,
407 AbD serotec, Atlanta, GA), anti-FLAG (F-3165, Sigma-Aldrich), anti-YTHDF1 (ab99080,
408 Abcam), anti-YTHDF2 (ABE542, EMD Millipore, Billerica, MA), anti-YTHDF3 (ab103328,
409 Abcam), and anti-HIV-1 p24 (AIDS Reagent Program, catalog # 6458). Cells were harvested and

410 lysed in cell lysis buffer (Cell Signaling, Beverly, MA) supplemented with the protease inhibitor
411 cocktail (Sigma-Aldrich). Immunoblotting was performed and ImageJ software (NIH) was used
412 to calculate the densitometry of immunoblotting bands as described [13].
413
414 **AlphaScreen assay.** Recombinant glutathione-S-transferase (GST)-tagged Y1-3 proteins were
415 purified as described [8]. Two RNA fragments, control RNA and m^6A-modified RNA (m^6A
416 RNA), corresponding to 235-281 nt containing the second GGACU consensus sequence, were
417 synthesized (Integrated DNA Technologies), and the RNA fragments were modified with biotin
418 at both 5' and 3' ends. Control RNA has no m^6A modification, while m^6A RNA fragment has
419 m^6A modification in GGACU motif. To eliminate RNA dimerization, the DIS sequence
420 (AAGCGCGC) was substituted with nucleotides GAG as described in a previous study [43].
421 AlphaScreen assays were conducted as previously reported with minor modifications [20].
422 Proteins and RNA fragments were diluted with AlphaScreen buffer (100 mM NaCl, 1 mM
423 $MgCl_2$, 1 mM DTT, 1 mg/mL BSA, 25 mM Tris pH 7.5). For the binding of proteins and
424 acceptor beads, Y1-3 proteins (25 nM) and acceptor beads (catalog # AL110C, 1:100 dilution;
425 PerkinElmer) were mixed and adjusted to 30 µL, and incubated at 4 °C for 2 h. For RNA and
426 donor bead binding, control or m^6A RNA (50 nM) were mixed with donor beads (catalog #
427 6760002S, 1:100 dilution; PerkinElmer) in 10 µL volume, and incubated at 4 °C for 2 h. After
428 the incubation, the protein and RNA were mixed, and incubated at 4 °C for 1 h. Samples (25 µL)
429 were added to microplate and read with EnSpire multimode plate reader (PerkinElmer).
430
431 ***In vitro* pull-down assays for RNA and Y1-3 protein binding.** Streptavidin Dynabeads M-280
432 (Invitrogen, catalog # 11205D) was used in this experiment. Beads were washed and incubated

433 with biotin-labeled m^6A RNA or control RNA at 4 °C for 60 min according to the
434 manufacturer's instructions, and purified Y1-3 proteins were added at concentrations of 1, 5, 25,
435 125, and 625 nM and incubated for 60 min. After washing, proteins bound to beads were eluted
436 for immunoblotting using specific antibodies to Y1, Y2, or Y3.
437
438 **qPCR assays.** To quantify HIV-1 gRNA after infection of HeLa/Y1-3 cells, at 1, 3 and 6 h after
439 viral infection, cells were collected and total RNAs were extracted with an RNeasy Mini kit
440 (Qiagen). Reverse transcription was conducted with first-strand synthesis (Invitrogen). qPCR
441 was used to measure HIV-1 gRNA as described [44]. To quantify HIV-1 early and late RT
442 products after viral infection, cellular DNA was extracted using a QIAamp DNA Blood Mini kit
443 (Qiagen). Early RT products were quantified using primers ert2f (5'-GTGCCC
444 GTCTGTTGTGTGAC-3') and ert2r (5'-GGCGCCACTGCTAGAGATTT-3'). Late RT
445 products were quantified using primers LW59 and LW60 as described [13]. GAPDH levels were
446 also quantified to normalize early and late RT data [13].
447
448 **IP of Y1-3 proteins to detect the interactions with HIV-1 proteins.** HEK293T cells (1×10^6)
449 were co-transfected with 2 μg pNL4-3 and 2 μg empty vector (pPB-CAG) or constructs
450 expressing individual HA-tagged Y1-3 proteins as previously described [13]. At 48 h post-
451 transfection, cells were harvested, lysed in 1% digitonin and total protein concentration was
452 quantified. To elucidate the effects of RNAs in Gag and Y1-3 interactions, one aliquot of each
453 cell lysate was treated with RNase A (100 μg/mL) for 1 h at room temperature, and IP was
454 conducted as described [45]. Proteins bound to anti-HA agarose beads were eluted by boiling in

455 sample buffer for immunoblotting. HIV Immunoglobulin (HIV-IG, NIH AIDS Reagent Program,
456 catalog # 3957) [25] was used to detect HIV-1 proteins precipitated by Y1-3 proteins.
457
458 **Prediction of the secondary structure of HIV-1 RNA segments**. The secondary RNA
459 structures of HIV-1 5'UTR segments from WT HIV-1 or mutants were predicted using online
460 mfold program according to the user's instruction (http://unafold.rna.albany.edu/?q=mfold).
461
462
463 **Statistical analyses.** Mann Whitney test was used to analyze AlphaScreen signal for m^6A and
464 control RNA fragment binding to Y1-3 proteins (Fig. 4C). Dunnett's multiple comparison test
465 was used for statistical analysis of all other data as indicated in figure legends. $P < 0.05$ is
466 considered significant.
467
468 **Acknowledgments**
469 We thank Dr. Vineet KewalRamani for sharing reagents, Dr. Corine St. Gelais for critical
470 reading the manuscript, and the Wu lab members for valuable discussions. The following
471 reagents were obtained through the NIH AIDS Reagent Program, Division of AIDS, NIAID,
472 NIH: HIV-1 p24 Gag Monoclonal (#24-3) from Dr. Michael H. Malim; HIV-IG (catalog #3957)
473 from NABI and NHLBI; TZM-bl from Dr. John C. Kappes, Dr. Xiaoyun Wu and Tranzyme Inc.
474
475 **Ethics approval and consent to participate**: Not applicable
476
477 **Consent for publication:** Not applicable

478

479 **Competing interests**

480 The authors declare that they have no competing interests.

481

482 **Funding**

483 This work was supported by a grant (GM128212) from the National Institutes of Health (NIH) to

484 L.W. L.W. was also supported in part by NIH grants (AI120209 and AI104483). M.K. was

485 supported by NIH grant AI062520. The funders had no role in study design, data collection and

486 analysis, decision to publish, or preparation of the manuscript.

487

488 **Author contributions**

489 Conceived and designed the experiments: WL, NT, MK, LW. Performed the experiments: WL,

490 NT, PCK. Analyzed the data: WL, NT, PCK, MK, CH, LW. Provided key reagents (purified

491 recombinant Y1-3 proteins): CL. Wrote the paper: WL, NT, MK, LW.

492

493

494 **References**

495 1. Wei CM, Gershowitz A, Moss B: Methylated nucleotides block 5' terminus of HeLa cell
496 messenger RNA. Cell 1975, 4:379-86.

497 2. Roundtree IA, Evans ME, Pan T, He C: Dynamic RNA Modifications in Gene
498 Expression Regulation. Cell 2017, 169:1187-200.

499 3. Li F, Zhao D, Wu J, Shi Y: Structure of the YTH domain of human YTHDF2 in complex
500 with an m(6)A mononucleotide reveals an aromatic cage for m(6)A recognition. Cell Res
501 2014, 24:1490-2.

502 4. Meyer KD, Jaffrey SR: The dynamic epitranscriptome: N6-methyladenosine and gene
503 expression control. Nat Rev Mol Cell Biol 2014, 15:313-26.

504 5. Fu Y, Dominissini D, Rechavi G, He C: Gene expression regulation mediated through
505 reversible m(6)A RNA methylation. Nat Rev Genet 2014, 15:293-306.

506 6. Sheth U, Parker R: Decapping and decay of messenger RNA occur in cytoplasmic
507 processing bodies. Science 2003, 300:805-8.

508 7. Meyer KD, Saletore Y, Zumbo P, Elemento O, Mason CE, Jaffrey SR: Comprehensive
509 analysis of mRNA methylation reveals enrichment in 3' UTRs and near stop codons. Cell
510 2012, 149:1635-46.

511 8. Wang X, Lu Z, Gomez A, Hon GC, Yue Y, Han D, Fu Y, Parisien M, Dai Q, Jia G, et al:
512 N6-methyladenosine-dependent regulation of messenger RNA stability. Nature 2014,
513 505:117-20.

514 9. Meyer KD, Patil DP, Zhou J, Zinoviev A, Skabkin MA, Elemento O, Pestova TV, Qian
515 SB, Jaffrey SR: 5' UTR m(6)A Promotes Cap-Independent Translation. Cell 2015,
516 163:999-1010.

517 10. Shi H, Wang X, Lu Z, Zhao BS, Ma H, Hsu PJ, He C: YTHDF3 facilitates translation
518 and decay of N6-methyladenosine-modified RNA. Cell Res 2017, 27:315-28.

519 11. Lichinchi G, Gao S, Saletore Y, Gonzalez GM, Bansal V, Wang Y, Mason CE, Rana
520 TM: Dynamics of the human and viral m(6)A RNA methylomes during HIV-1 infection
521 of T cells. Nat Microbiol 2016, 1:16011.

522 12. Kennedy EM, Bogerd HP, Kornepati AV, Kang D, Ghoshal D, Marshall JB, Poling BC,
523 Tsai K, Gokhale NS, Horner SM, Cullen BR: Posttranscriptional m(6)A Editing of HIV-1
524 mRNAs Enhances Viral Gene Expression. Cell Host Microbe 2016, 19:675-85.

525 13. Tirumuru N, Zhao BS, Lu W, Lu Z, He C, Wu L: N(6)-methyladenosine of HIV-1 RNA
526 regulates viral infection and HIV-1 Gag protein expression. Elife 2016, 5.

527 14. Antonucci JM, St Gelais C, de Silva S, Yount JS, Tang C, Ji X, Shepard C, Xiong Y,
528 Kim B, Wu L: SAMHD1-mediated HIV-1 restriction in cells does not involve
529 ribonuclease activity. Nat Med 2016, 22:1072-4.

530 15. St Gelais C, Roger J, Wu L: Non-POU Domain-Containing Octamer-Binding Protein
531 Negatively Regulates HIV-1 Infection in CD4(+) T Cells. AIDS Res Hum Retroviruses
532 2015, 31:806-16.

533 16. Fitzgerald KA, Palsson-McDermott EM, Bowie AG, Jefferies CA, Mansell AS, Brady G,
534 Brint E, Dunne A, Gray P, Harte MT, et al: Mal (MyD88-adapter-like) is required for
535 Toll-like receptor-4 signal transduction. Nature 2001, 413:78-83.

536 17. Fitzgerald KA, McWhirter SM, Faia KL, Rowe DC, Latz E, Golenbock DT, Coyle AJ,
537 Liao SM, Maniatis T: IKKepsilon and TBK1 are essential components of the IRF3
538 signaling pathway. Nat Immunol 2003, 4:491-6.

539 18. Wei CM, Moss B: Nucleotide sequences at the N6-methyladenosine sites of HeLa cell
540 messenger ribonucleic acid. Biochemistry 1977, 16:1672-6.

541 19. Dominissini D, Moshitch-Moshkovitz S, Schwartz S, Salmon-Divon M, Ungar L,
542 Osenberg S, Cesarkas K, Jacob-Hirsch J, Amariglio N, Kupiec M, et al: Topology of the
543 human and mouse m6A RNA methylomes revealed by m6A-seq. Nature 2012, 485:201-
544 6.

545 20. Kessl JJ, Kutluay SB, Townsend D, Rebensburg S, Slaughter A, Larue RC, Shkriabai N,
546 Bakouche N, Fuchs JR, Bieniasz PD, Kvaratskhelia M: HIV-1 Integrase Binds the Viral
547 RNA Genome and Is Essential during Virion Morphogenesis. Cell 2016, 166:1257-68
548 e12.

549 21. Telesnitsky A, Wolin SL: The Host RNAs in Retroviral Particles. Viruses 2016, 8.

550 22. Eckwahl MJ, Telesnitsky A, Wolin SL: Host RNA Packaging by Retroviruses: A Newly
551 Synthesized Story. MBio 2016, 7:e02025-15.

552 23. Derdeyn CA, Decker JM, Sfakianos JN, Wu X, O'Brien WA, Ratner L, Kappes JC, Shaw
553 GM, Hunter E: Sensitivity of human immunodeficiency virus type 1 to the fusion
554 inhibitor T-20 is modulated by coreceptor specificity defined by the V3 loop of gp120. J
555 Virol 2000, 74:8358-67.

556 24. Kharytonchyk S, Monti S, Smaldino PJ, Van V, Bolden NC, Brown JD, Russo E,
557 Swanson C, Shuey A, Telesnitsky A, Summers MF: Transcriptional start site
558 heterogeneity modulates the structure and function of the HIV-1 genome. Proc Natl Acad
559 Sci U S A 2016, 113:13378-83.

560 25. Cummins LM, Weinhold KJ, Matthews TJ, Langlois AJ, Perno CF, Condie RM, Allain
561 JP: Preparation and characterization of an intravenous solution of IgG from human
562 immunodeficiency virus-seropositive donors. Blood 1991, 77:1111-7.

563 26. Kutluay SB, Zang T, Blanco-Melo D, Powell C, Jannain D, Errando M, Bieniasz PD:
564 Global changes in the RNA binding specificity of HIV-1 gag regulate virion genesis. Cell
565 2014, 159:1096-109.

566 27. Krug RM, Morgan MA, Shatkin AJ: Influenza viral mRNA contains internal N6-
567 methyladenosine and 5'-terminal 7-methylguanosine in cap structures. J Virol 1976,
568 20:45-53.

569 28. Beemon K, Keith J: Localization of N6-methyladenosine in the Rous sarcoma virus
570 genome. J Mol Biol 1977, 113:165-79.

571 29. Canaani D, Kahana C, Lavi S, Groner Y: Identification and mapping of N6-
572 methyladenosine containing sequences in simian virus 40 RNA. Nucleic Acids Res 1979,
573 6:2879-99.

574 30. Ping XL, Sun BF, Wang L, Xiao W, Yang X, Wang WJ, Adhikari S, Shi Y, Lv Y, Chen
575 YS, et al: Mammalian WTAP is a regulatory subunit of the RNA N6-methyladenosine
576 methyltransferase. Cell Res 2014, 24:177-89.

577 31. Pollom E, Dang KK, Potter EL, Gorelick RJ, Burch CL, Weeks KM, Swanstrom R:
578 Comparison of SIV and HIV-1 genomic RNA structures reveals impact of sequence
579 evolution on conserved and non-conserved structural motifs. PLoS Pathog 2013,
580 9:e1003294.

581 32. Wilkinson KA, Gorelick RJ, Vasa SM, Guex N, Rein A, Mathews DH, Giddings MC,
582 Weeks KM: High-throughput SHAPE analysis reveals structures in HIV-1 genomic RNA
583 strongly conserved across distinct biological states. PLoS Biol 2008, 6:e96.

584 33. Abd El-Wahab EW, Smyth RP, Mailler E, Bernacchi S, Vivet-Boudou V, Hijnen M,
585 Jossinet F, Mak J, Paillart JC, Marquet R: Specific recognition of the HIV-1 genomic
586 RNA by the Gag precursor. Nat Commun 2014, 5:4304.

587 34. Liu N, Dai Q, Zheng G, He C, Parisien M, Pan T: N(6)-methyladenosine-dependent RNA
588 structural switches regulate RNA-protein interactions. Nature 2015, 518:560-4.

589 35. Gokhale NS, McIntyre AB, McFadden MJ, Roder AE, Kennedy EM, Gandara JA,
590 Hopcraft SE, Quicke KM, Vazquez C, Willer J, et al: N6-Methyladenosine in
591 Flaviviridae Viral RNA Genomes Regulates Infection. Cell Host Microbe 2016, 20:654-
592 65.

593 36. Lichinchi G, Zhao BS, Wu Y, Lu Z, Qin Y, He C, Rana TM: Dynamics of Human and
594 Viral RNA Methylation during Zika Virus Infection. Cell Host Microbe 2016, 20:666-73.

595 37. Ye F, Chen ER, Nilsen TW: Kaposi's Sarcoma-Associated Herpesvirus Utilizes and
596 Manipulates RNA N6-Adenosine Methylation To Promote Lytic Replication. J Virol
597 2017, 91:e00466-17.

598 38. Tan B, Liu H, Zhang S, da Silva SR, Zhang L, Meng J, Cui X, Yuan H, Sorel O, Zhang
599 SW, et al: Viral and cellular N(6)-methyladenosine and N(6),2'-O-dimethyladenosine
600 epitranscriptomes in the KSHV life cycle. Nat Microbiol 2018, 3:108-20.

601 39. Courtney DG, Kennedy EM, Dumm RE, Bogerd HP, Tsai K, Heaton NS, Cullen BR:
602 Epitranscriptomic Enhancement of Influenza A Virus Gene Expression and Replication.
603 Cell Host Microbe 2017, 22:377-86.

604 40. Dong C, Kwas C, Wu L: Transcriptional restriction of human immunodeficiency virus
605 type 1 gene expression in undifferentiated primary monocytes. J Virol 2009, 83:3518-27.

606 41. Wang JH, Janas AM, Olson WJ, KewalRamani VN, Wu L: CD4 coexpression regulates
607 DC-SIGN-mediated transmission of human immunodeficiency virus type 1. J Virol 2007,
608 81:2497-507.

609 42. Wang JH, Kwas C, Wu L: Intercellular adhesion molecule 1 (ICAM-1), but not ICAM-2
610 and -3, is important for dendritic cell-mediated human immunodeficiency virus type 1
611 transmission. J Virol 2009, 83:4195-204.

612 43. Keane SC, Heng X, Lu K, Kharytonchyk S, Ramakrishnan V, Carter G, Barton S, Hosic
613 A, Florwick A, Santos J, et al: Structure of the HIV-1 RNA packaging signal. Science
614 2015, 348:917-21.

615 44. Dong C, Janas AM, Wang JH, Olson WJ, Wu L: Characterization of human
616 immunodeficiency virus type 1 replication in immature and mature dendritic cells reveals
617 dissociable cis- and trans-infection. J Virol 2007, 81:11352-62.

618 45. St Gelais C, de Silva S, Hach JC, White TE, Diaz-Griffero F, Yount JS, Wu L:
619 Identification of cellular proteins interacting with the retroviral restriction factor
620 SAMHD1. J Virol 2014, 88:5834-44.

621

622

623 **Figure Legends**

624

625 **Fig. 1 Overexpression of Y1-3 proteins inhibits HIV-1 infection through decreasing HIV-1**
626 **gRNA and viral reverse transcription. (A)** Overexpression of Y1-3 proteins in HeLa/Y1-3 cell
627 lines. **(B)** Cells were infected with HIV-1 Luc/VSV-G (MOI=1), and viral infection was
628 measured by luciferase activity at 24 h post-infection (hpi) (n=3 independent experiments, same
629 in the following). **(C)** Quantified HIV-1 gRNA levels after infection of HeLa/Y1-3 cells and
630 vector control cells (n=3). **(D)** Early reverse transcription (RT) product levels at 6, 12 and 24 hpi
631 (n=3). **(E)** Late RT product levels at 6, 12 and 24 hpi (n=3). Results are shown as mean ± SEM.
632 Dunnett's multiple comparison test was used to determine statistical significance. * $P < 0.05$, ***
633 $P < 0.0005$, compared each group with vector control cells in each corresponding experiment.
634 Data are from at least 3 independent experiments with biological duplicates.

635

636 **Fig. 2 Overexpression of Y1-3 proteins in HeLa/CD4 target cells inhibits wild-type HIV-1**
637 **replication. (A)** Surface levels of CD4 (exogenous) and CXCR4 (endogenous) in HeLa/CD4
638 cells overexpressing individual Y1-3 proteins or vector control cells were analyzed by flow
639 cytometry. Isotype-matched IgG was used as a negative control for immunostaining. The
640 numbers on the top of the plots indicate the percentages of CD4- and CXCR4-positive cells. **(B-**
641 **F)** HeLa/CD4 cells overexpressing individual Y1-3 proteins were infected with HIV-1_{NL4-3}
642 (MOI=1) for 72 h. **(B)** HIV-1 Gag protein expression and over-expression of FLAG-tagged Y1-3
643 proteins in HeLa/CD4 cells were confirmed by immunoblotting. **(C)** ELISA quantification of
644 HIV-1 p24 levels in the supernatants from infected cells. **(D** and **E)** qPCR quantification of the
645 levels of HIV-1 early RT products (D) and late RT products (E). **(F)** RT-qPCR quantification of
646 HIV-1 *gag* mRNA in the cells. (C-F) The reverse transcriptase inhibitor nevirapine (NVP) was
647 used to treat vector cells as a negative control for HIV-1 infection. All results are shown as mean
648 ± SEM (n=3) and data presented are representative of 3 independent experiments. Dunnett's
649 multiple comparison test was used to determine statistical significance. ** P <0.005 and *** P
650 <0.0005 compared with vector control cells.
651
652 **Fig. 3 Y1-3 proteins specifically bind to HIV-1 gRNA in infected HeLa/CD4 cells.** (**A**)
653 Immunoblotting of Y1-3 in the input and immunoprecipitation (IP) samples from HeLa/CD4
654 cells infected with HIV-1. HeLa/CD4 cells stably overexpressing FLAG-tagged Y1-3 proteins,
655 MAL (MyD88 adapter-like protein), or empty vector control cells were infected with HIV-1_{NL4-3}
656 at an MOI of 5 for 3 h. FLAG antibodies were used to immunoprecipitate Y1-3 proteins or MAL
657 in HeLa/CD4 cells after HIV-1 infection. (**B**) HIV-1 gRNA is bound by Y1-3 proteins expressed
658 in HeLa/CD4 cells. HIV-1 infection of HeLa/CD4 cells overexpressing Y1-3 proteins, MAL, or

659 empty vector control cells as described above in (A). Cell lysates were immunoprecipitated with
660 anti-FLAG antibody, and HIV-1 *gag* RNA levels were quantified by RT-qPCR. Dunnett's
661 multiple comparison test was used to determine statistical significance. *** P <0.0005 compared
662 with the vector control cells. Data presented are representative of 4 independent experiments.
663
664 **Fig. 4 Purified recombinant Y1-3 proteins preferentially bind to an m^{6}A-modifed HIV-1**
665 **RNA fragment *in vitro*. (A)** Structure of partial HIV-1 RNA 5' UTR containing two GGACU
666 motifs (in gray background) that are labeled with blue words *m^{6}A #1* (nt. 195-199) and *m^{6}A #2*
667 (nt. 239-243). PBS and DIS are highlighted in bold. The figure is adapted from Kharytonchyk et
668 al. [24]. **(B)** Sequences of synthesized control (Ctrl) RNA and m^{6}A-modified (m^{6}A RNA)
669 fragment containing the second GGACU motif (in bold) in HIV-1 RNA 5' UTR corresponding
670 to nt. 235-281. The DIS-containing sequence (AA**GCGCGC**) was replaced with nucleotides
671 GAG (underlined) to eliminate RNA dimerization. The A* indicates the m^{6}A modification site in
672 the RNA fragment. **(C)** Binding of Y1-3 proteins to m^{6}A RNA versus control, unmodified RNA
673 was monitored using the AlphaScreen assay. Data are from two independent experiments with
674 biological triplicates. Results are shown as mean ± SEM. ** P < 0.005 by Mann Whitney test.
675 **(D)** Y1-3 protein pull-down using biotin-labeled control and m^{6}A RNA fragments. Streptavidin
676 Dynabeads were used in the pull-down assay and immunoblotting was performed using specific
677 antibodies to Y1, Y2, or Y3. **(E)** Y1-3 protein pull-down level based on densitometry analysis of
678 the bands in immunoblotting. Data are average results from two independent experiments. (**F**)
679 Calculated concentrations of Y1-3 proteins needed to reach 50% pull-down levels of 625 nM
680 Y1-3 by the m^{6}A RNA fragment.
681

682 **Fig. 5 A to G mutations in GGACU motifs of the 5' UTR of HIV-1 gRNA reduce viral**
683 **infectivity. (A)** Schematic representation of introduced mutations in the 5' UTR region of HIV-1
684 proviral DNA. **(B)** Gag protein expression in HEK293T cell lysates expressing wild type (WT)
685 and mutants (Mut1-3). The relative p24 levels were normalized based on GAPDH levels. **(C)**
686 HIV-1 p24 levels in the supernatants at 48 h post-transfection were quantified by ELISA (n=3).
687 **(D)** Infectivity of WT and mutant HIV-1 was quantified by measuring luciferase activity 48 h
688 after infection of TZM-bl cells (n=4). Results are shown as mean ±SEM. Dunnett's multiple
689 comparison test was used for statistical analysis. *** $P < 0.0005$, compared HIV-1 mutants to
690 WT virus. **(E)** Endogenous Y1-3 proteins in TZM-bl cells were knocked down by combined Y1-
691 3 specific siRNA transfection. Immunoblotting confirms Y1-3 knockdown compared with
692 control siRNA-transfected cells. **(F)** The infectivity of WT and mutant HIV-1 was quantified by
693 measuring luciferase activity 48 h after infection of TZM-bl target cells (n=4). Results are shown
694 as mean ±SEM. Dunnett's multiple comparison test was used for statistical analysis. * $P<0.05$,
695 compared HIV-1 mutants with WT HIV-1. **(G)** Predicted secondary structures of the RNA
696 segments containing the PBS (left two panels) or DIS (right two panels, sequences are
697 highlighted in bold) of WT, Mut1 and Mut2 viruses. Two A to G mutation sites (Mut1 and
698 Mut2) are circled and pointed by blue arrows.
699
700 **Fig. 6 Knockdown of Y1-3 proteins in virus-producing cells affects HIV-1 Gag expression,**
701 **viral production and infectivity. (A)** Immunoblotting of HEK293T cells with siRNA-mediated
702 single Y1-3 knockdown or Y1-3 combined knockdown and pNL4-3 transfection. (**B**) ELISA
703 quantification of p24 levels in supernatants from the siRNA-transfected HEK293T cells (n=4).
704 **(C)** Infectivity of HIV-1 generated in control cells, or cells with individual Y1-3 knockdown or

705 combined knockdown was quantified by measuring luciferase activity 48 h after infection of
706 TZM-bl reporter cells (n=3). Results are shown as mean ± SEM. Dunnett's multiple comparison
707 tests were used for statistical analysis. **P<0.005, *** P<0.0005, compared Y1-3 specific
708 siRNA knockdown with non-specific control (Ctrl) siRNA.
709
710 **Fig. 7 Y1-3 proteins and HIV-1 Gag form a complex with RNAs in HIV-1-infected target**
711 **cells.** HEK293T cells were co-transfected with pNL4-3 and individual plasmids expressing HA-
712 and FLAG-tagged Y1-3 or empty vector. Cell lysates were treated with or without RNase A (100
713 μg/mL) before immunoprecipatation (IP) of Y1-3 proteins using anti-HA agarose beads. The
714 input or IP products of HIV-1 Gag or CA (p24) were detected using HIV Immunoglobulin.
715 Expression and IP of Y1-3 were confirmed with anti-FLAG immunoblotting. Results presented
716 are representative of three independent experiments.

717 **Table 1. Sequences of siRNAs used for Y1-3 knockdown**

Targets	Catalog numbers (QIAGEN)	Target sequences (5'- 3')
YTHDF1	SI00764715	CCGCGTCTAGTTGTTCATGAA
YTHDF1	SI04240117	CCCTCCACCCATAAAGCATAA
YTHDF1	SI04240418	TACGGACAGCTCAGTAACGGA
YTHDF1	SI04279121	CAGGCTGGAGAATAACGACAA
YTHDF2	SI00764757	AAGGACGTTCCCAATAGCCAA
YTHDF2	SI04270777	TTCGGTCCATTAATAACTATA
YTHDF3	SI00764778	ATGGATTAAATCAGTATCTAA
YTHDF3	SI04133339	TAAGTCAAAGAAGACGTATTA
Negative Control	SI03650325	AATTCTCCGAACGTGTCACGT

718

Fig. 1

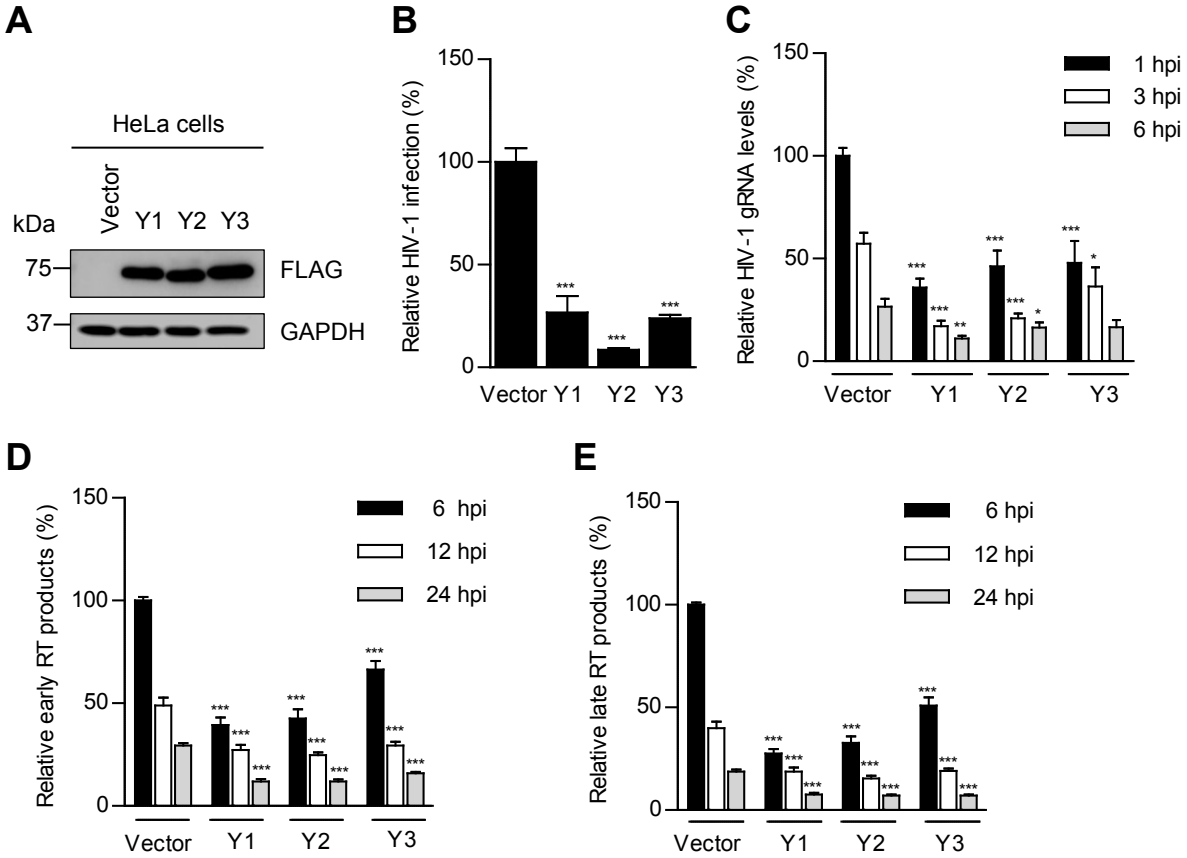
A
HeLa cells
Vector
Y1
Y2
Y3
kDa
75
37
FLAG
GAPDH
B
Relative HIV-1 infection (%)
150
100
50
0
Vector
Y1
Y2
Y3
C
Relative HIV-1 gRNA levels (%)
1 hpi
3 hpi
6 hpi
D
Relative early RT products (%)
6 hpi
12 hpi
24 hpi
E
Relative late RT products (%)

Fig. 2

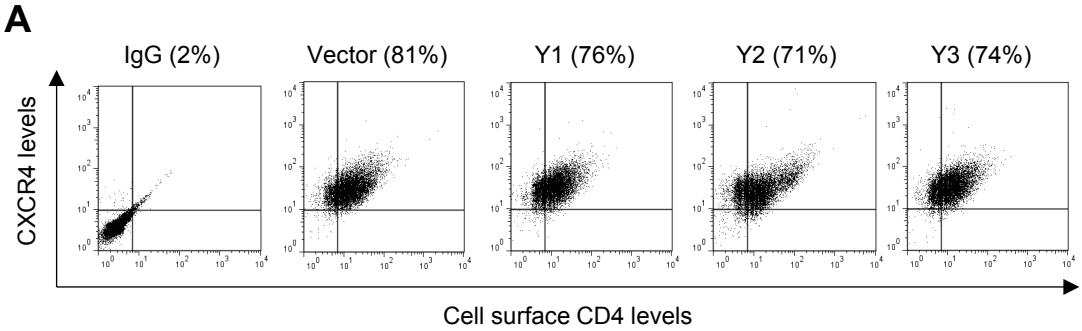
A
IgG (2%)
Vector (81%)
Y1 (76%)
Y2 (71%)
Y3 (74%)
CXCR4 levels
Cell surface CD4 levels

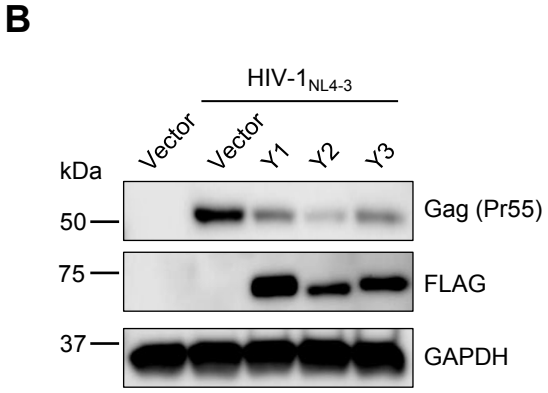
B
HIV-1NL4-3
Vector
Vector
Y1
Y2
Y3
kDa
50
75
37
Gag (Pr55)
FLAG
GAPDH

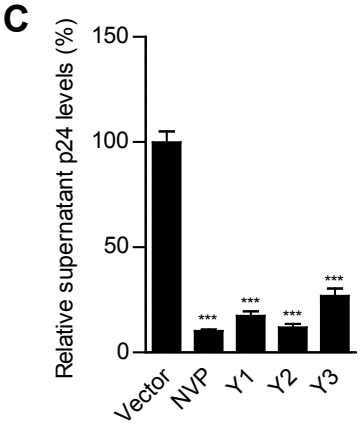
C
Relative supernatant p24 levels (%)
150
100
50
0
Vector
NVP
Y1
Y2
Y3

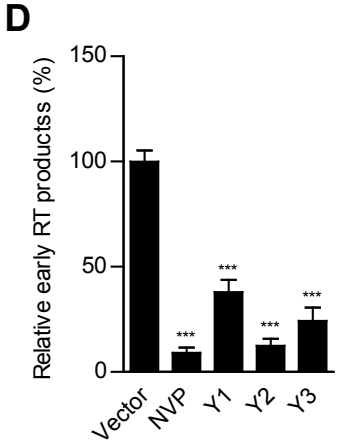
D
Relative early RT productss (%)
150
100
50
0
Vector
NVP
Y1
Y2
Y3

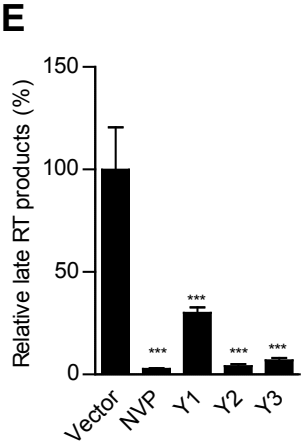
E
Relative late RT products (%)
150
100
50
0
Vector
NVP
Y1
Y2
Y3

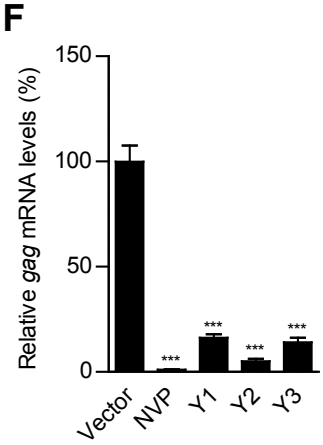
F
Relative gag mRNA levels (%)
150
100
50
0
Vector
NVP
Y1
Y2
Y3

Fig. 3

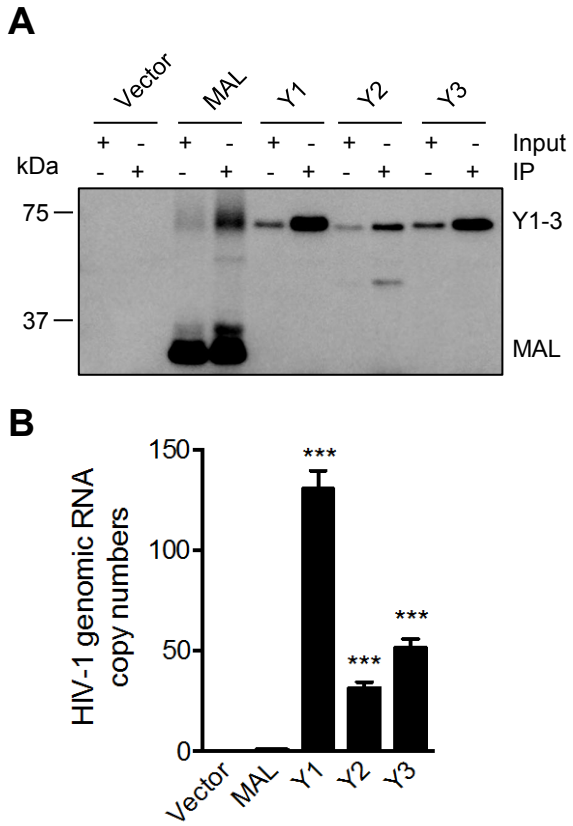
A
Vector
MAL
Y1
Y2
Y3
Input
IP
kDa
75
37
Y1-3
MAL
B
HIV-1 genomic RNA copy numbers
150
100
50
0
***
***
***
Vector
MAL
Y1
Y2
Y3

Fig. 4

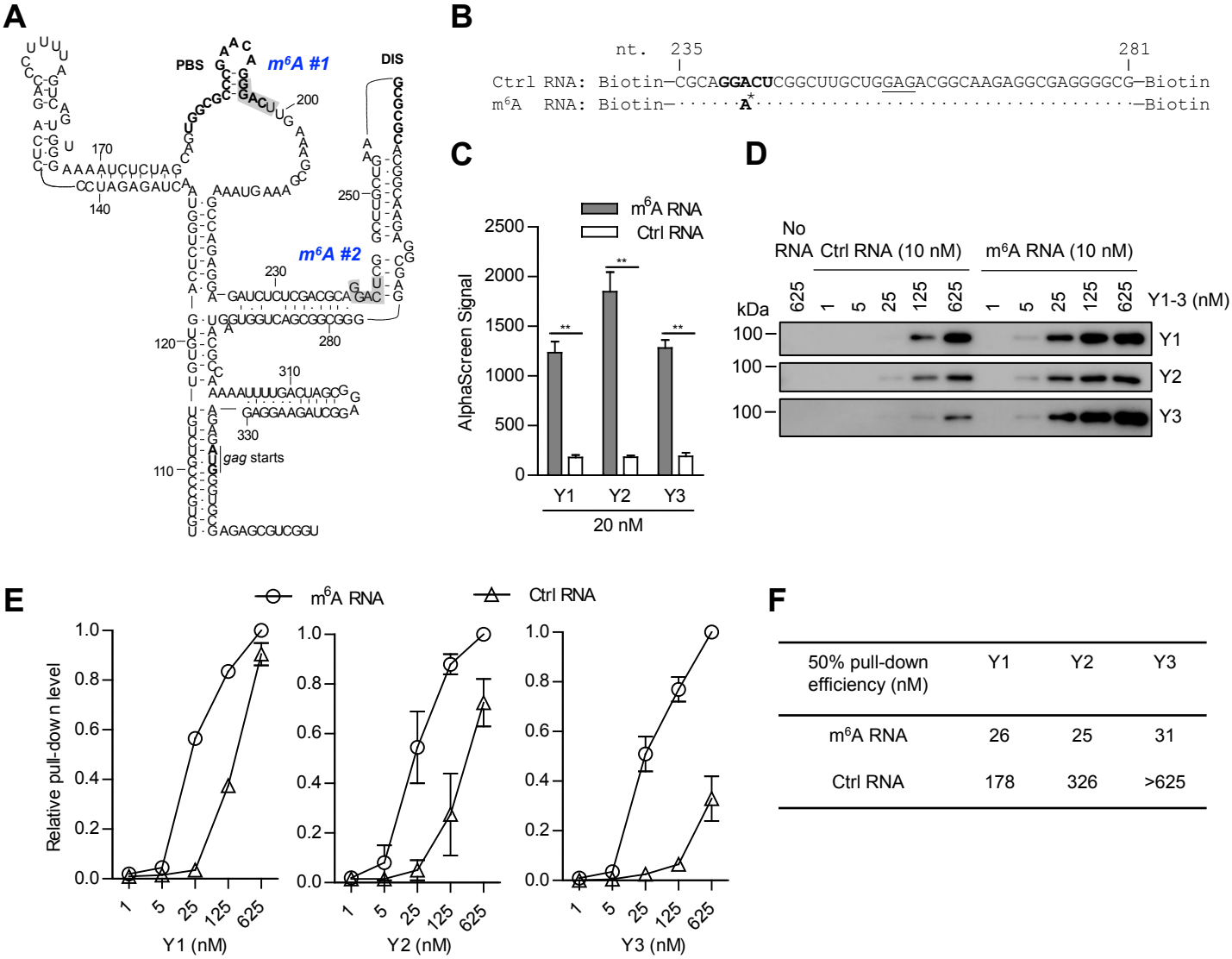

50% pull-down efficiency (nM)	Y1	Y2	Y3
m6A RNA	26	25	31
Ctrl RNA	178	326	>625

Fig. 5

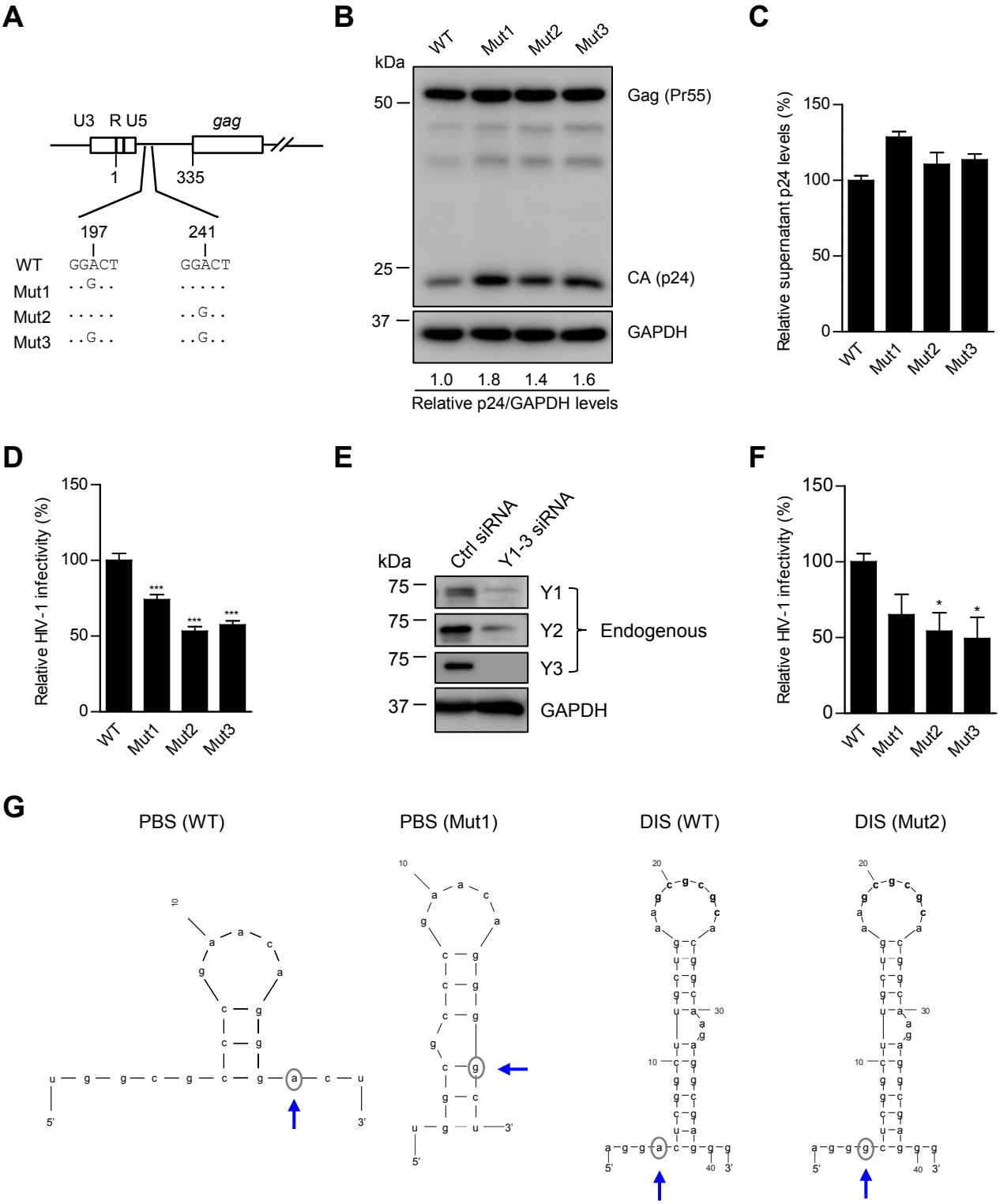
A
U3 R U5
gag
1
335
197
241
WT GGACT GGACT
Mut1 ..G.. .....
Mut2 ....G..
Mut3 ..G.. ..G..
B
WT Mut1 Mut2 Mut3
kDa
50
25
37
Gag (Pr55)
CA (p24)
GAPDH
1.0 1.8 1.4 1.6
Relative p24/GAPDH levels
C
Relative supernatant p24 levels (%)
150
100
50
0
WT Mut1 Mut2 Mut3
D
Relative HIV-1 infectivity (%)
150
100
50
0
***
***
***
WT Mut1 Mut2 Mut3
E
Ctrl siRNA
Y1-3 siRNA
kDa
75
75
75
37
Y1
Y2
Y3
Endogenous
GAPDH
F
Relative HIV-1 infectivity (%)
150
100
50
0
*
*
WT Mut1 Mut2 Mut3
G
PBS (WT)
PBS (Mut1)
DIS (WT)
DIS (Mut2)
5'
3'

Fig. 6

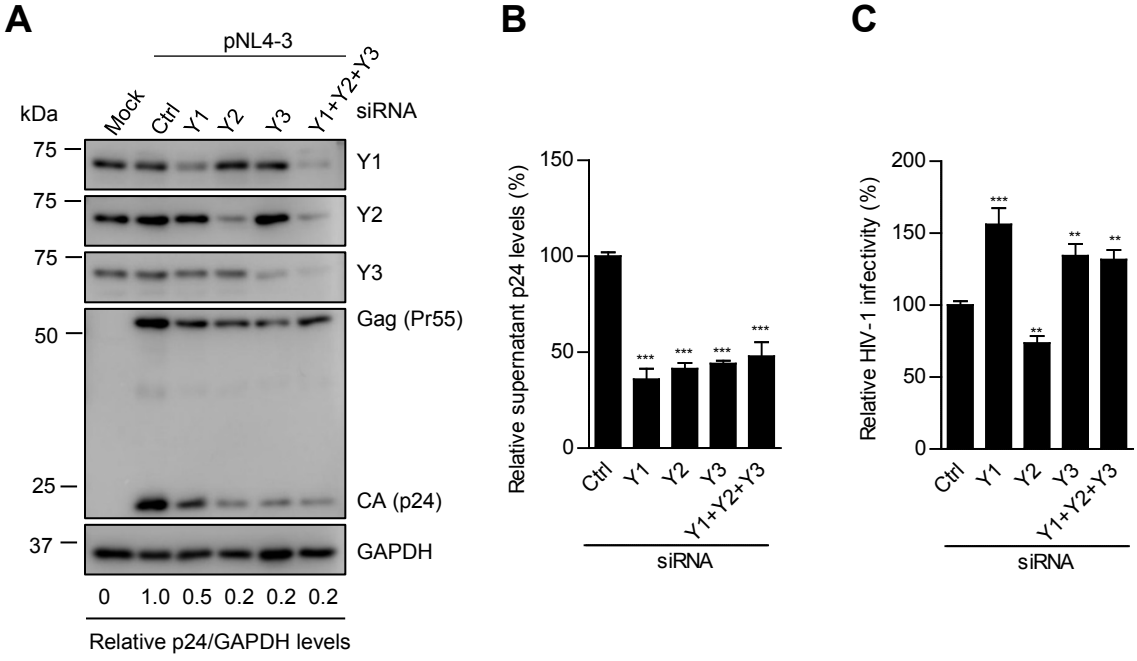
A
pNL4-3
kDa
Mock
Ctrl
Y1
Y2
Y3
Y1+Y2+Y3
siRNA
75
75
75
50
25
37
Y1
Y2
Y3
Gag (Pr55)
CA (p24)
GAPDH
0 1.0 0.5 0.2 0.2 0.2
Relative p24/GAPDH levels
B
Relative supernatant p24 levels (%)
150
100
50
0
***
Ctrl
Y1
Y2
Y3
Y1+Y2+Y3
siRNA
C
Relative HIV-1 infectivity (%)
200
150
100
50
0
***
**
Ctrl
Y1
Y2
Y3
Y1+Y2+Y3
siRNA

Fig. 7

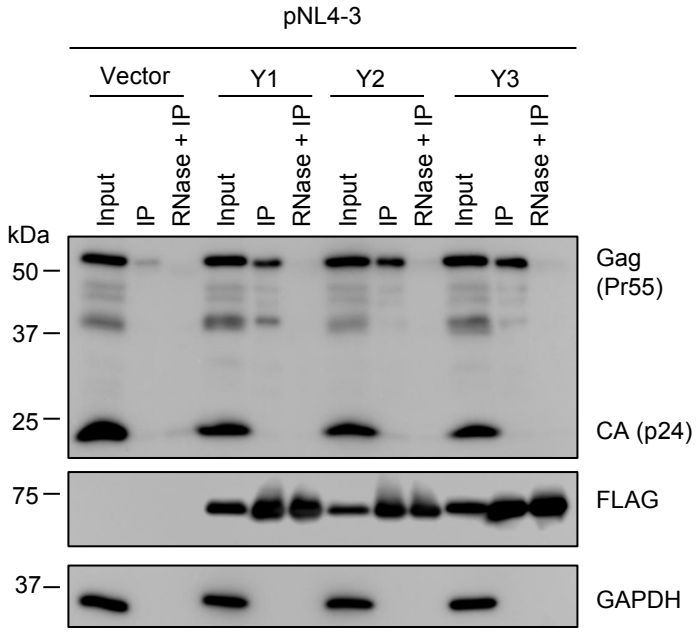
pNL4-3
Vector
Y1
Y2
Y3
Input
IP
RNase + IP
Input
IP
RNase + IP
Input
IP
RNase + IP
Input
IP
RNase + IP
kDa
50
37
25
75
37
Gag
(Pr55)
CA (p24)
FLAG
GAPDH